COMMUNICATIONS CHEMISTRY

ARTICLE

https://doi.org/10.1038/s42004-019-0244-y OPEN

Controlled deprotection and release of a small molecule from a compartmented synthetic tissue module

Michael J. Booth [1]*, Idil Cazimoglu [1] & Hagan Bayley[1]

Synthetic tissues built from communicating aqueous droplets offer potential applications in biotechnology, however, controlled release of their contents has not been achieved. Here we construct two-droplet synthetic tissue modules that function in an aqueous environment. One droplet contains a cell-free protein synthesis system and a prodrug-activating enzyme and the other a small-molecule prodrug analog. When a Zn^{2+}-sensitive protein pore is made in the first droplet, it allows the prodrug to migrate from the second droplet and become activated by the enzyme. With Zn^{2+} in the external medium, the activated molecule is retained in the module until it is released on-demand by a divalent cation chelator. The module is constructed in such a manner that one or more, potentially with different properties, might be incorporated into extended synthetic tissues, including patterned materials generated by 3D-printing. Such modules will thereby increase the sophistication of synthetic tissues for applications including controlled multidrug delivery.

[1] Chemistry Research Laboratory, University of Oxford, Oxford OX1 3TA, UK. *email: michael.booth@chem.ox.ac.uk

When aqueous droplets are submerged in a lipid-containing oil, they form lipid monolayers on their surfaces. When two such droplets are brought together they form a droplet interface bilayer (DIB)[1]. These DIBs can be functionalised with membrane proteins, such as nanopores and proton pumps[2]. Networks of these droplets can be constructed manually[2] or automatically using microfluidics[3] or 3D-printing[4]. Droplet networks have been developed into electronic devices[5], chemical[6–8] and biochemical reactors[2,9–12] and tissue-mimics[4].

To fully utilise the potential applications of droplet networks in biotechnology, for instance in drug delivery, they must function in an external aqueous environment. Simple aggregates of aqueous droplets, formed from emulsions, have previously been prepared and approved for clinical use as slow release drug delivery vehicles[13]. Recently, more functionally complex multicompartment lipid-bounded structures have been generated that exist in aqueous media. For example, multisomes, aqueous droplet networks within a lipid-containing oil drop in an external aqueous environment, have been generated manually[14], with microfluidics[15] and by 3D-printing[4]. Controlled fusion of all the internal compartments with the external solution has been demonstrated with temperature- and pH-sensitive lipids[4]. Molecular and ionic transfer through aqueous-bounded multicompartment structures has been demonstrated[14–18]. Cascades of different reactions have been enabled by shuttling intermediate molecules through the multicompartment structures by using both the membrane pore protein α-hemolysin (αHL) and membrane-permeant intermediates[16]. However, as the external membrane was also permeablized by αHL, the starting materials, intermediates and products were moving into the external solution while they were reacting internally.

A vital development would be the ability to controllably permeabilize the external membranes, while keeping the internal membranes permeable. This would allow reactions to occur internally, before release of the products upon demand. The difficulty in this originates from the use of pore proteins, such as αHL, to shuttle molecules across internal membranes; αHL will insert into both the internal and external membranes, leaving them both permeable. Heptakis(2,3,6-tri-O-methyl)-β-cyclodextrin (TRIMEB) has been added to block αHL and achieve controlled permeabilization of single compartment vesicles[19], but TRIMEB did not completely block leakage. TRIMEB has also been used with multicompartment structures assembled from vesicles, to block leakage to the external environment and therefore allow transfer across between the compartments[20]. In this case, transfer was measured over only 10 min, no internal reactions were performed, and any leakage to the external solution was not assayed. In addition, these multicompartment structures are fundamentally different to those used in the present work, as they have double bilayers between each compartment, whereas here we have single bilayers.

We have previously generated droplet networks from synthetic cells (aqueous compartments) that contained an in vitro transcription/translation (IVTT) system. We demonstrated controlled synthesis of αHL from a light-activated DNA template, which mediated the movement of ions and small molecules across a DIB[21,22]. The release of small molecules from multicompartment lipid-bounded structures into an external aqueous environment has also been demonstrated with αHL generated by IVTT[23]. However, again, no control over the permeability of the internal versus the external membrane was achieved.

To achieve the selective permeabilization of the internal bilayers of a multicompartment structure in aqueous solution, while keeping the external bilayers impermeable, we utilised a previously developed divalent cation-sensitive αHL mutant, αHL-4H[24]. αHL-4H contains four histidine mutations at residues 123, 125, 133 and 135 on each subunit, forming a divalent cation binding tetrad at the end of the barrel of the pore. Electrical recordings on the αHL-4H homoheptamer showed that only 10 μM Zn^{2+} is required to efficiently block the pore, and that EDTA reopens it. These conditions are biocompatible, as shown when the related αHL-H5 was used to selectively permeabilize mammalian cells[25].

Here, we have generated two-droplet synthetic tissue modules in an aqueous solution, where lipid bilayers separate the internal compartments, and the compartments and the external environment. To demonstrate the advantage of the selective permeabilization of the internal bilayer of a functional module, while keeping the external bilayers impermeable, we aimed to perform an in situ reaction by transferring a reagent from one droplet to an enzyme in the other droplet. The product would then be trapped within the module for an extended time, prior to release. Within the synthetic tissue modules, we compartmentalised DNA encoding αHL-4H, an IVTT system, and an activating enzyme, β-galactosidase in one droplet and a galactose-protected fluorogenic substrate in another, with Zn^{2+} in the external solution (Fig. 1). Following protein pore expression and membrane insertion, the substrate moved into the first droplet, where it was cleaved by the enzyme. The fluorophore was trapped within the two lipid-bounded compartments, until the external bilayers were permeabilized by activating the externally oriented αHL-4H pores with a chelating agent. The work demonstrates a fundamental level of control not previously implemented in multicompartment structures.

Results

Testing droplet permeability with αHL-4H. The homoheptameric αHL-4H protein pore can spontaneously insert into a lipid bilayer and does not allow ionic current flow in the presence of 10 μM Zn^{2+} [24]. We set out to determine whether the movement of a small molecule across the DIB of a droplet pair in a lipid-containing oil could be similarly blocked. We have previously cloned the αHL gene into the PURExpress control template (CT)[21], for IVTT using the PURExpress system, an *E. coli*-based cell-free expression kit[26]. This αHL construct was mutated by using homologous recombination to insert four His residues at positions 123, 125, 133 and 135, to generate αHL-4H. As both His codons have similar rates of usage in *E. coli*[27], we used both CAT (123 and 125) and CAC (133 and 135). The polymerase chain reaction was then carried out to produce linear αHL-4H DNA templates for IVTT. After IVTT, we added the fluorescent glucose derivative 2-[N-(7-nitrobenz-2-oxa-1,3-diazol-4-yl) amino]-2-deoxy-D-glucose (NBDG) to the pre-expressed αHL-4H, diluting the reaction mix by a half. Droplets (50 nL) of this mix were produced in a lipid-containing oil, using a pipette, along with 50 nL droplets of either 20 μM $ZnCl_2$ or 5 mM EDTA, using a 0.5 μL syringe. Droplet pairs, partitioned by DIBs, were prepared from αHL-4H/NBDG droplets with (1) $ZnCl_2$ droplets or (2) EDTA droplets (Supplementary Fig. 1a–d). Following pore insertion into the DIB, Zn^{2+} was expected to block the movement of NBDG into the neighbouring droplet (Supplementary Fig. 1a, b), while NBDG would move freely between the two droplets when EDTA was present (Supplementary Fig. 1c, d). The droplet pairs were incubated for 4 h and imaged by confocal microscopy. The mean fluorescence intensity across each of the droplets was calculated (Supplementary Fig. 1e). As expected, when EDTA was present in the neighbouring droplet, NBDG passed through the αHL-4H pores and equilibrated across the two droplets. By contrast, when $ZnCl_2$ was in the neighbouring droplet, we observed <1% transfer. This demonstrates that DIBs can be permeabilized with αHL-4H and that the αHL-4H pore can be blocked by Zn^{2+}.

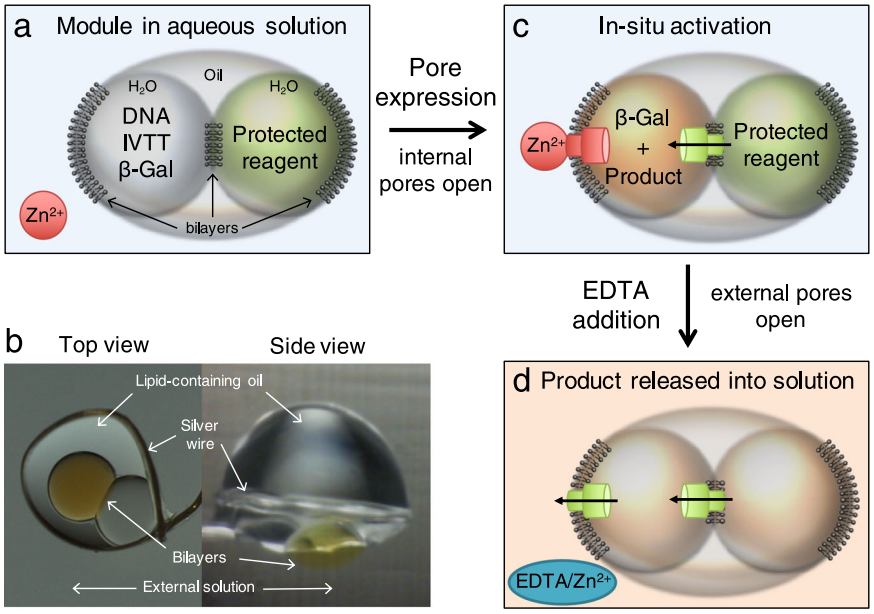

Fig. 1 In situ reaction and controlled release from a synthetic tissue module. a We aimed to generate functional modules in an external aqueous environment, where lipid bilayers separated each internal compartment, and the compartments and the external environment. **b** Image of a module suspended on a Teflon-coated silver wire in an external aqueous solution. The lipid-containing oil drop contains two aqueous droplets, with or without the fluorescent glucose derivative NBDG. The droplets have formed bilayers with each other (top view) and the external solution (side view). Teflon-coated silver wires, 76 μm in diameter. **c** In this work we aimed to encapsulate DNA encoding a divalent cation-sensitive protein pore (αHL-4H), an IVTT system, and an activating enzyme, β-galactosidase (β-Gal) within one droplet and a protected substrate molecule in the other. Pore expression would initiate transfer of the reagent into the β-Gal-containing droplet. The use of the αHL-4H pore would permeabilize the internal bilayer, while keeping the external bilayers impermeable, because the pores in them would be blocked by external Zn^{2+} ions. This selective bilayer permeabilization would trap the reagents and the products of the enzyme cleavage within the synthetic tissue module. **d** The external bilayers could then be permeabilized by using a chelating agent (EDTA), allowing product release into the external aqueous environment.

Selective bilayer permeabilization between droplets in oil. We next aimed to demonstrate selective permeabilization by αHL-4H by expressing the protein within an IVTT droplet in a 3-droplet chain in lipid-containing oil (Fig. 2 and Supplementary Fig. 2). In the above experiment (Supplementary Fig. 1) we halved the concentration of the IVTT mix following expression, which produced for more stable bilayers. However, little protein was expressed at this dilution. A vital goal of the three-droplet experiment experiment (Fig. 2) was to stabilise the DIBs to a higher concentration of the IVTT system, to maximise the rate of small molecule transfer, by the expressed αHL-4H. Previously, we have used 10% PEGylated lipids with 1,2-diphytanoyl-sn-glycero-3-phosphocholine (DPhPC) to achieve bilayer stability[21]. However, under these conditions we observed slow transfer rates, e.g., when WT αHL had been expressed for 18 h, the small molecule dye, TAMRA, remained unequilibrated in a droplet pair. This most likely arose from a low rate of insertion of the αHL pore into the membrane due to steric hinderance from the PEGylated head groups. Therefore, we tested new lipid combinations to obtain good stability with higher protein insertion rates. When we diluted the IVTT mix in a droplet to two-thirds of its original concentration, we found that a mixture of 60:40 1-palmitoyl-2-oleoyl-glycero-3-phosphocholine (POPC):DPhPC, in 60:40 silicone oil:hexadecane, achieved a good balance between bilayer stability (stronger with higher POPC concentration) and small molecule transfer rates (faster with lower POPC concentration). POPC was chosen for testing here as it has been regularly used for vesicle formation. We assume the increase in stability arises from more favourable lipid packing in the bilayer due to the unsaturated tail, compared to the fully saturated DPhPC tail. This stability may then decrease pore insertion. This lipid-containing oil mixture was used in the rest of the experiments detailed here.

We used our three-droplet chains to demonstrate transfer rates (Fig. 2 and Supplementary Fig. 2). The central droplet D2 of the three droplet chains, generated in the POPC:DPhPC lipid-containing oil, contained the IVTT mix and DNA encoding αHL-4H, so upon expression the pore would insert into the two DIBs formed by D2 (Fig. 2a and Supplementary Fig. 2a). One droplet connected to D2 contained NBDG and EDTA, while the other contained Zn^{2+}. The two DIBs formed by D2 therefore mimic the internal and external membranes of a synthetic tissue module (Fig. 1), where the NBDG and IVTT droplets are "internal compartments", and the Zn^{2+}-containing droplet acts as the "external solution". Upon αHL-4H expression and membrane insertion, we expected the NBDG to move into the IVTT droplet, because the pore is open in the presence of EDTA. However, NBDG should remain trapped in D1 and D2 and not move into the third Zn^{2+}-containing droplet D3 (Fig. 2a and Supplementary Fig. 2a). The 3-droplet chains were prepared from 50 nL droplets and observed with wide-field fluorescence microscopy. We found that the NBDG equilibrated between D1 and D2 over 6 h (Fig. 2b and Supplementary Fig. 2b), much faster than we had previously demonstrated[21]. This time includes αHL-4H expression, membrane insertion, and small molecule movement. Over this 6 h period we observed no movement of NBDG into D3, which contained Zn^{2+}, mimicking the external solution in the synthetic tissue module design.

We then reformed the 3-droplet chain with D1 and D2, both again 50 nL, but with a 200 nL Zn^{2+}-containing droplet D3, to better mimic a large external solution volume. These droplet chains were examined by confocal microscopy at 0 and 18 h (Fig. 2c and Supplementary Fig. 3). As expected, we again observed full equilibration of NBDG between D1 and D2, and ≤1% movement into D3. These experiments demonstrate distinct

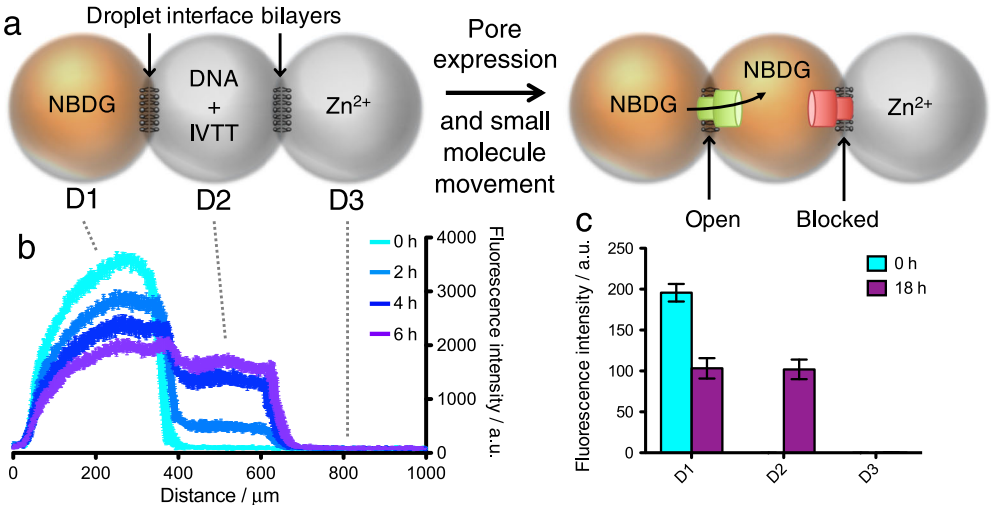

Fig. 2 Testing selective DIB permeabilization by αHL-4H between droplets in oil. a Three droplets were prepared in a lipid-containing oil, containing a fluorescent glucose derivative NBDG (D1), DNA encoding αHL-4H and the IVTT system (D2), and $ZnCl_2$ (D3). By connecting D1 and D3 to either side of D2, droplet interface bilayers were formed. **b** Measurement of the fluorescence intensity across the droplet chain during expression of αHL-4H demonstrates insertion of the protein into the bilayers and the transfer of NBDG into D2, but not into D3 ($n = 4$). **c** Droplet chains were left for 18 h and still no transfer to D3 was observed ($n = 4$). Error bars represent one standard deviation.

bilayer permeability differences between two DIBs formed by the same droplet.

Selective bilayer permeabilization in synthetic tissue modules. The majority of work on droplet networks has been carried out in a surrounding oil solution, as performed in the previous sections (Fig. 2). Following these experiments, we aimed to demonstrate the use of αHL-4H in multisome-based synthetic tissue modules, aqueous droplets in a lipid-containing oil drop surrounded by an aqueous environment. To do this we produced two-droplet modules manually by suspending the lipid-containing oil drop on a silver wire loop within a custom-made chamber[14]. We used a Teflon-coated silver wire, which adhered to the less dense oil droplet. The oil droplet easily fell off non-coated wires. Chambers were filled with 1 mL of external solution containing 20 µM $ZnCl_2$. A lipid-containing oil drop (~1 µL) was suspended on the wire in the centre of the chamber. Two 50 nL droplets were first incubated in lipid-containing oil for at least 20 min, and then pipetted into the lipid-containing oil drop, where bilayers formed between the two droplets and between each droplet and the external solution (Fig. 1b).

We generated synthetic tissue modules (Fig. 3) based on the pilot studies (Fig. 2). Two different droplets were produced, one containing the IVTT mix and DNA encoding αHL-4H and the other NBDG and EDTA. These were incubated in a lipid-containing oil, then transferred into an oil drop suspended in an external aqueous Zn^{2+} solution. Following bilayer formation, a synthetic tissue module was formed (Fig. 3a, d, e). Upon αHL-4H pore formation, we expected the NBDG to move into the IVTT droplet, but remain trapped with the module due to the external Zn^{2+} (Fig. 3b). Only following the addition of EDTA to the external solution would the trapped NBDG be released (Fig. 3c). The two-droplet modules were incubated for 18 h. With bright field imaging, we observed the equilibration of the NBDG between the two internal compartments (Fig. 3d, e). Following this, either extra buffer (Fig. 3d) or 500 µM EDTA (final concentration) (Fig. 3e) was added to the external solution and the modules were incubated for an additional 6 h. Bright field imaging showed that no change occurred after buffer addition. However, when EDTA was added, NBDG release from the IVTT droplet was observed. It was expected that the NBDG would be released from the IVTT droplet, because this droplet was the only one with pores that directly accessed the external solution. These experiments were also carried out without any DNA (Supplementary Fig. 4). As expected, bright field imaging demonstrated no NBDG transfer or release under these conditions, as no pore protein was expressed.

In addition to bright field imaging, 100 µL of the external solution was removed from each module's chamber at 18 h, and after the further 6 h following the addition of buffer or EDTA. The fluorescence of these 100 µL aliquots was measured and converted to nM NBDG by using a calibration curve (Fig. 3f). With no DNA present, release was below the limit of detection (LOD) of the assay, which was 15 nM. As 3 mM NBDG was held within the original 50 nL droplet, 100% release into the 1 mL external solution would give 150 nM NBDG; therefore, the LOD was equivalent to 10% release. When DNA was present in the IVTT droplet of the module, after 18 h no significant difference in released NBDG was observed by comparison with the no DNA controls. Following the addition of EDTA to the external solution and incubation for a further 6 h, the release of NBDG was detected (55 ± 3%). However, when only extra buffer was added, we saw no significant increase in NBDG detected, which remained below the LOD. This demonstrated the efficient trapping of NBDG within the αHL-4H-expressing synthetic tissue module over extended periods of time in the presence of external Zn^{2+}, and the ability to selectively permeabilize the external membrane, and release the internal contents, by the addition of EDTA. Due to instability of the bilayers, prolonged incubation of synthetic tissue modules to observe the full release of trapped molecules was not possible.

In-situ substrate turnover and controlled release from a synthetic tissue module. An advantage of multicompartment structures over single compartments is the ability to separate a reagent and an activator and subsequently effect activation by mixing of the compartments' contents. Following the successful demonstration of on-demand permeabilization of the external membrane of a two-compartment lipid-bounded structure, we sought to activate a reagent within αHL-4H synthetic tissue modules and then trigger the release of the product (Fig. 4).

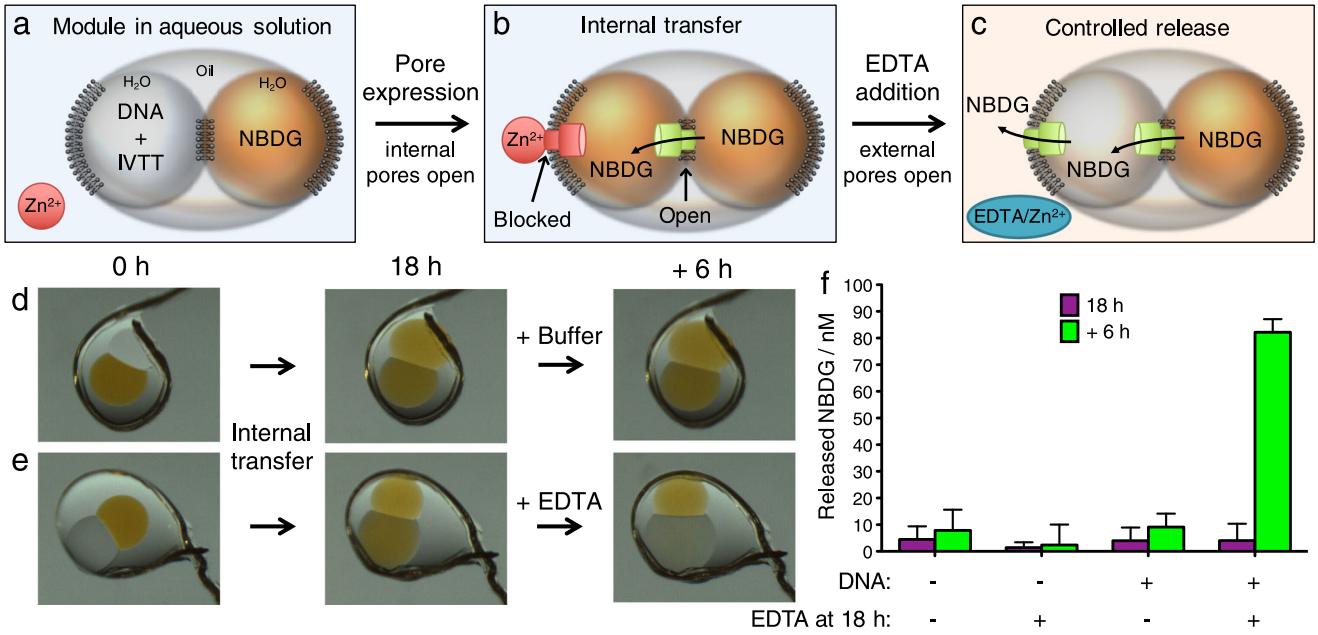

Fig. 3 Controlled release of small molecules from a synthetic tissue module. a Two-droplet modules, in which one droplet contained DNA encoding αHL-4H and the IVTT system, and the second NBDG, were generated in an aqueous solution containing $ZnCl_2$. **b** The αHL-4H protein pore was expressed and inserted into both internal and external membranes. The open internal pores allowed the movement of NBDG into the IVTT droplet. The presence of external Zn^{2+} blocked the pores in the external membrane and trapped the NBDG within the module. **c** Addition of the chelator (EDTA) to the external solution mediated the release of NBDG into the external solution. **d**, **e** Images of synthetic tissue modules as described in (**a**). Following transfer and trapping of the NBDG for 18 h, the NBDG can either remain trapped (**d**) or be released with EDTA (**e**). Teflon-coated silver wires, 76 μm in diameter. **f** Quantification of NBDG in the external solution of functional modules containing αHL-4H DNA or no DNA, with or without the addition of EDTA after 18 h ($n \geq 4$ in each condition). NBDG was released only when DNA was present and EDTA added after 18 h of incubation. Error bars represent one standard deviation.

To achieve this, we used the well-studied β-galactosidase (β-Gal) enzyme[28]. This is a medically-relevant activating enzyme; many pro-drugs have been generated that contain glucose or galactose protecting groups[29]. We generated modules that contained two droplets, an IVTT droplet with the IVTT mix and DNA encoding αHL-4H and a droplet containing 3-carboxyumbelliferyl β-D-galactopyranoside (CUG) (Fig. 4a). CUG is a non-fluorescent small molecule that is converted into the fluorescent 7-hydroxycoumarin-3-carboxylic acid (HCCa) by β-Gal (Fig. 4b). Therefore, in our modules, we expected that, upon expression and insertion of αHL-4H into the internal and external membranes, CUG would equilibrate into the IVTT droplet containing β-Gal, but remain trapped in the internal compartments due to presence of Zn^{2+} in the external solution. This would allow in situ activation to occur and the product would also remain trapped in the functional module (Fig. 4c).

These two-droplet synthetic tissue modules were formed, along with controls without DNA or without β-Gal. A 100 μL sample of the external solution was removed from each module chamber at 18 h, and after a further 6 h following the addition of extra buffer or EDTA. The concentration of HCCa in the external solution was measured by fluorescence spectroscopy (Fig. 4d). As 25 mM CUG was held within the original 50 nL droplet, 100% enzymatic activation and 50% release (as expected from Fig. 3) into the 1 mL external solution would give 625 nM HCCa. Without DNA, no fluorescence in the external solution was detected after 18 h or after the addition of EDTA and a further 6 h. Without β-Gal, <0.5% HCCa was detected at 18 h, and 1.2% HCCa was detected after the addition of EDTA and further 6 h incubation. This was likely due to a low background fluorescence signal from CUG and/or a small amount of uncatalyzed hydrolysis to HCCa over the course of the experiment. When both DNA and β-Gal were present, a small increase in fluorescence was observed after 18 h (1.8% of the original CUG). Following the addition of EDTA to the external solution and incubation for a further 6 h, a large increase in fluorescence was detected (19 ± 3% of the original CUG, giving a 38% reaction yield assuming 50% release). This indicated that the in-situ reaction had occurred and had trapped the product within the module until controlled release was initiated. When buffer alone was added to these modules at 18 h, no significant increase in fluorescence output was observed after a further 6 h, indicating prolonged trapping of the product within the synthetic tissue module.

Discussion

We have demonstrated the ability to carry out enzymatic substrate conversions within multicompartment lipid-bounded structures, and trap the contents internally with Zn^{2+}, and then, using a chelator, release the trapped molecules on-demand into the external aqueous solution. It remains to be seen whether multicompartment structures with divalent cation-sensitive αHL pores will function in the presence of living cells, however, the pores themselves function under physiological conditions[25]. One major advantage of multicompartment structures is the ability to separate incompatible components into different compartments. As many small molecules inhibit IVTT, this separation allows the use of very high concentrations of any payload molecules. For example, in the present work, mM concentrations of small molecules were held separately from the functional IVTT droplet. This allowed us to detect the release of a molecule from a single nL-sized multicompartment structure in 1 mL of external solution. In the future, this will give high local delivery concentrations during drug delivery. The separation will also allow use of

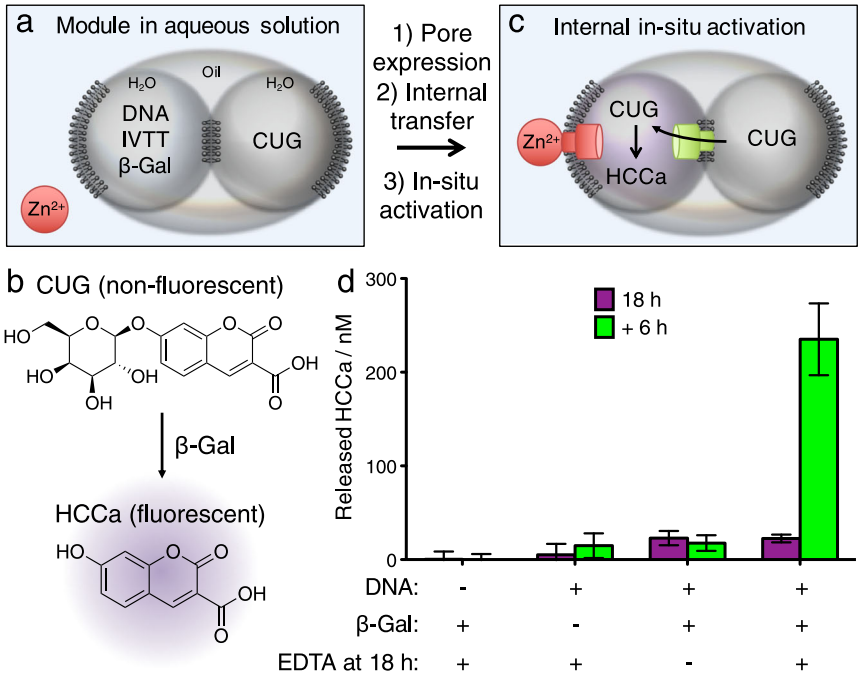

Fig. 4 In situ activation and controlled release from a synthetic tissue module. a Two-droplet modules, in which one droplet contains DNA encoding αHL-4H, the IVTT system, and β-galactosidase (β-Gal) and the second 3-carboxyumbelliferyl-β-D-galactopyranoside (CUG), were generated in an aqueous solution containing $ZnCl_2$. Following αHL-4H expression and internal transfer of CUG, the β-Gal cleaved the CUG to form 7-hydroxycoumarin-3-carboxylic acid (HCCa). **b** β-Gal produces the fluorescent HCCa from the non-fluorescent CUG. **c**, **d** Quantification of HCCa from the external solution of modules with or without αHL-4H DNA or β-Gal ($n \geq 4$ in each condition). HCCa was released only when both DNA and β-Gal were present and EDTA added after 18 h of incubation. Error bars represent one standard deviation.

reagents that would otherwise inhibit IVTT, such as DNA intercalators or protein binders.

Current functional lipid-bounded multicompartment structures, including ours, suffer from instability to fusion. Previously, simple two-compartment structures have been generated with ~80% yield and a 60-min lifetime[30] and structures containing IVTT machinery with 12% yield (lifetime not given)[31]. We have improved upon this to allow ~50–60% survival after 24 h, with minimal handling. However, stability issues have limited the scope of our current work. For instance, prolonged incubation of synthetic tissue modules to observe the full release of trapped molecules was not possible. Current research is working towards increasing the stability, including the use of hydrogel coatings[32] and the production of smaller structures by using 3D-printing[4] and microfluidics[23]. However, a higher number of smaller constructs would be required to release the same payload as the larger structures described here. More engineering work is required to fully realise the potential of these multicompartment structures, especially with regards to their use with living cells. As the functionality developed here is based around the protein pore, and not the specific type of multicompartment structure or its method of formation, we envisage its application more widely for multicompartment structures.

The technology we have developed here, to controllably release trapped contents from multicompartment structures under biocompatible conditions, is an important step towards developing smart lipid-bilayer bounded devices for use in drug delivery and sensing applications. Our αHL-4H functional modules could also be incorporated into larger synthetic tissues to control internal reactions.

Methods

DNA sequences. All DNA was purchased from Sigma.

Cloning an αHL-4H gene into the PURExpress Control Template. The αHL-4H gene was constructed in the PURExpress CT by using homologous recombination[33], starting from the previously cloned αHL gene[21]. Primers (Table 1) were designed that overlap the desired region of mutation (4H FRW and 4H REV) and the end of the gene (CT-HL FRW and CT-HL REV). The αHL plasmid was digested with BamHI to form a linear fragment before polymerase chain reaction (PCR) amplifications.

Two PCRs were carried out for homologous recombination, with Phusion high-fidelity DNA polymerase (NEB) master mix: (1) 4H FRW + CT-HL REV and (2) 4H REV and CT-HL FRW. PCRs were made according to the manufacturer's protocol in a total of 10 µL with 2.5 µL of each primer (10 µM stock) and 1.5 ng of digested plasmid as template. The following thermal cycle was performed for both PCRs: 98 °C for 30 s, 35× (98 °C for 10 s, 55 °C for 30 s, 72 °C for 90 s), 72 °C for 5 min.

PCR products were not purified before homologous recombination. XL-10 Gold competent *Escherichia coli* cells (NEB) were thawed on ice for 30 min. A 2 µL of PCR product 1 and 0.5 µL of PCR product 2 were added to 40 µL cells, and the mixture was held on ice for an additional 30 min. The cells were then heat shocked for 30 s at 42 °C, then held on ice for 2 min, and plated on LB Agar plates containing ampicillin (100 µg/mL). Colonies were grown in LB containing ampicillin (100 µg/mL) and the plasmids purified with Thermo GeneJet Plasmid Miniprep kits. Sequences were verified with Sanger sequencing (Source BioScience) using the primers CT Seq FRW and CT Seq REV (Table 1).

PCR of αHL-4H to generate linear PURExpress template. The linear DNA template was constructed by PCR, using primers CT FRW and CT REV (Table 1) and the αHL-4H plasmid digested with HindIII, with Phusion high-fidelity DNA polymerase (NEB) master mix. PCRs were made according to the manufacturer's protocol in a total of 50 µL with 5 µL of each primer (10 µM) and 1 ng of digested plasmid. The following thermal cycle was performed: 98 °C for 30 s, 35× (98 °C for 10 s, 55 °C for 30 s, 72 °C for 45 s), 72 °C for 10 min.

Table 1 Sequences of DNAs used.

DNA name	DNA sequence
4H FRW	GGTGATGATACAGGAAAAATTCACGGCCACATTGGTGCAAATGTTTCG
4H REV	AATTTTTCCTGTATCATCACCATGAACATGACCGTTGAATCCATAAG
CT-HL FRW	GAAATGACAAATTAATGAGGATCCCGGGAATTCTCGAGTAAGG
CT-HL REV	GAATTCCCGGGATCCTCATTAATTTGTCATTTCTTC
CT FRW	GAAATTAATACGACTCACTATAGGGTCTAG
CT REV	GATATAGTTCCTCCTTTCAG
CT Seq FRW	GCTAGTGGTGCTAGCCCCGC
CT Seq REV	GGGACCGCTAGCGCGGCCGC

The PCR products were purified with Thermo GeneJet PCR kits and the DNA precipitated overnight at −80 °C by the addition of sodium acetate (1/10 volume, 3 M) followed by ethanol (3 volumes). A DNA pellet was recovered by centrifugation at 16,000 rcf for 30 min and washed twice with ice-cold 80% v/v ethanol. The DNA pellet was then dried in a Speed Vac Concentrator (Savant), and resuspended in 10 mM Tris-HCl, pH 8.0.

PURExpress IVTT in bulk. IVTT for protein expression was performed with the PURExpress In Vitro Protein Synthesis kit (NEB, E6800) according to the manufacturer's protocol with the addition of Murine RNAse Inhibitor (NEB, MB0314). DNA was added to a final concentration of 5 ng/μL. Final reaction volumes were 5 μL. The reactions were held at 37 °C for 3 h.

PURExpress IVTT in droplets and synthetic tissue modules. IVTT for droplet experiments was performed with the PURExpress In Vitro Protein Synthesis kit (NEB, E6800) with the addition of Murine RNAse Inhibitor (NEB, MB0314). DNA was added to a final concentration of 10 ng/μL. These reactions were prepared in a volume of 2.5 μL, which was then diluted with water to a final volume of 3.75 μL. When using β-Gal (*E. coli*, Sigma), the enzyme was added to a final concentration of 2 U/mL. Reactions were held on ice until droplets were generated.

Fluorescence microscopy. A Leica SP5 instrument was used for confocal fluorescence microscopy, with a 514 nm laser. A Leica DMi8 instrument was used for wide-field fluorescence microscopy, with a green fluorescent protein filter cube. All fluorescence images were analysed by using Fiji (ImageJ). Any brightness or contrast changes made to the images were the same within any image set.

Preparation of lipids. Lipid films comprising a 60% molar fraction of POPC (Avanti) with DPhPC (Avanti, 4ME 16:0 PC) were prepared, dried overnight in a desiccator, and stored under N_2 at −80 °C. Lipid films were suspended, on the day of each experiment, in 60:40 silicone:hexadecane, at a total concentration of 1 mM and sonicated in a sonication bath for 25 min prior to use.

Droplet formation. Droplets (50 or 200 nL) were formed as previously described[21] in the lipid-containing oil within poly(methyl methacrylate) (PMMA) wells, by using a 0.5 μL syringe (Hamilton, 7000.5 KH) or a 10 μL pipette with a gel loading tip (for all PURExpress droplets). When using the pipette, ~1 μL droplets were initially made and then drawn into a new gel loading tip using the capillary force. The new tip was then immersed back into the lipid-containing oil solution and a finger pressed against the opposite end of the tip until a small amount of the solution protruded from the end. This droplet was separated from the pipette tip by bringing the tip out of the solution.

When using pre-expressed αHL-4H (Supplementary Fig. 2), the reactions were diluted by half with an NBDG solution (final concentration of 250 μM). The neighbouring droplets contained MES buffer pH 6.5 (50 mM), NaCl (267 mM) and either EDTA (5 mM) or $ZnCl_2$ (20 μM).

PURExpress reactions for droplets or synthetic tissue modules were used as prepared. The neighbouring droplets contained PURExpress solution A (1/3.75 dilution), NaCl (130 mM), and different combinations of EDTA (5 mM in all experiments apart from 2 mM in Fig. 4), $ZnCl_2$ (20 μM), NBDG (250 μM, Fig. 2; 3 mM, Fig. 3) and/or CUG (25 mM) as stated in the text.

Synthetic tissue module formation. Chambers were formed by gluing (Araldite 2-part epoxy) the bottom section of a plastic cuvette (Fisher) to a glass cuvette. Then a 2–3 cm long Teflon-coated silver wire (A-M Systems, diameter 0.003″ bare and 0.0055″ coated) was glued to the edge. After overnight drying, the wire was bent into a loop, which was located in the centre of the chamber. The chambers were washed with water and ethanol, and left to dry in air prior to use.

A 1 mL solution of MES pH 6.5 (50 mM), NaCl (267 mM) and $ZnCl_2$ (20 μM) was added to each chamber. Lipid-containing oil drops (~1 μL) were added to the Teflon-coated silver wires, zapped with an anti-static gun, and left to form a monolayer for 10 min. Droplets formed in a separate PMMA well containing the lipid in oil (incubated for at least 20 min), were then added to the oil drop with a pipette and left for 5 min to form bilayers. The modules were held at 25 °C.

Aliquots of 100 μLs were taken from the external solution for analysis at time points indicated in the text. Of these aliquots, 95 μL were analysed by a Tecan Infinite M1000 Pro fluorescence plate reader. An excitation wavelength of 465 nm and emission wavelength of 540 nm were used for NBDG, and an excitation wavelength of 360 nm and emission wavelength of 450 nm were used for HCCa. Then in total 100 μL of buffer (MES and NaCl only) or EDTA (MES, NaCl and 5 mM EDTA—500 μM final concentration) was added back into the chambers.

Data availability

The authors declare that all data supporting the findings of this study are available within the article and its supplementary information files. Additional data related to this study can be obtained from the corresponding authors upon request.

Received: 30 August 2019; Accepted: 25 November 2019;
Published online: 12 December 2019

References

1. Booth, M. J., Restrepo Schild, V., Downs, F. G. & Bayley, H. Functional aqueous droplet networks. *Mol. BioSyst.* **13**, 1658–1691 (2017).
2. Holden, M. A., Needham, D. & Bayley, H. Functional bionetworks from nanoliter water droplets. *J. Am. Chem. Soc.* **129**, 8650–8655 (2007).
3. Elani, Y., deMello, A. J., Niu, X. & Ces, O. Novel technologies for the formation of 2-D and 3-D droplet interface bilayer networks. *Lab Chip* **12**, 3514–3520 (2012).
4. Villar, G., Graham, A. D. & Bayley, H. A tissue-like printed material. *Science* **340**, 48–52 (2013).
5. Maglia, G. et al. Droplet networks with incorporated protein diodes show collective properties. *Nat. Nanotechnol.* **4**, 437–440 (2009).
6. Guzowski, J., Gizynski, K., Gorecki, J. & Garstecki, P. Microfluidic platform for reproducible self-assembly of chemically communicating droplet networks with predesigned number and type of the communicating compartments. *Lab Chip* **16**, 764–772 (2016).
7. Jones, G., King, P. H., Morgan, H., de Planque, M. R. & Zauner, K. P. Autonomous droplet architectures. *Artif. Life* **21**, 195–204 (2015).
8. Thutupalli, S. & Herminghaus, S. Tuning active emulsion dynamics via surfactants and topology. *Eur. Phys. J. E. Soft Matter* **36**, 91 (2013).
9. Carreras, P. et al. A microfluidic platform for size-dependent generation of droplet interface bilayer networks on rails. *Biomicrofluidics* **9**, 64121 (2015).
10. Carreras, P., Law, R. V., Brooks, N., Seddon, J. M. & Ces, O. Microfluidic generation of droplet interface bilayer networks incorporating real-time size sorting in linear and non-linear configurations. *Biomicrofluidics* **8**, 54113 (2014).
11. Yasuga, H. et al. Logic gate operation by DNA translocation through biological nanopores. *PLoS ONE* **11**, e0149667 (2016).
12. Dupin, A. & Simmel, F. C. Signalling and differentiation in emulsion-based multi-compartmentalized in vitro gene circuits. *Nat. Chem.* **11**, 32–39 (2019).
13. Angst, M. S. & Drover, D. R. Pharmacology of drugs formulated with DepoFoam: a sustained release drug delivery system for parenteral administration using multivesicular liposome technology. *Clin. Pharmacokinet.* **45**, 1153–1176 (2006).
14. Villar, G., Heron, A. J. & Bayley, H. Formation of droplet networks that function in aqueous environments. *Nat. Nanotechnol.* **6**, 803–808 (2011).
15. Elani, Y., Solvas, X. C., Edel, J. B., Law, R. V. & Ces, O. Microfluidic generation of encapsulated droplet interface bilayer networks (multisomes) and their use as cell-like reactors. *Chem. Commun.* **52**, 5961–5964 (2016).

16. Elani, Y., Law, R. V. & Ces, O. Vesicle-based artificial cells as chemical microreactors with spatially segregated reaction pathways. *Nat. Commun.* **5**, 5305 (2014).
17. Deng, N. N., Yelleswarapu, M., Zheng, L. & Huck, W. T. Microfluidic assembly of monodisperse vesosomes as artificial cell models. *J. Am. Chem. Soc.* **139**, 587–590 (2017).
18. Wang, X. et al. Chemical communication in spatially organized protocell colonies and protocell/living cell micro-arrays. *Chem. Sci.* **10**, 9446–9453 (2019).
19. Thomas, J. M., Friddin, M. S., Ces, O. & Elani, Y. Programming membrane permeability using integrated membrane pores and blockers as molecular regulators. *Chem. Commun.* **53**, 12282–12285 (2017).
20. Bolognesi, G. et al. Sculpting and fusing biomimetic vesicle networks using optical tweezers. *Nat. Commun.* **9**, 1882 (2018).
21. Booth, M. J., Restrepo Schild, V., Graham, A. D., Olof, S. N. & Bayley, H. Light-activated communication in synthetic tissues. *Sci. Adv.* **2**, e1600056 (2016).
22. Booth, M. J., Restrepo Schild, V., Box, S. J. & Bayley, H. Light-patterning of synthetic tissues with single droplet resolution. *Sci. Rep.* **7**, 9315 (2017).
23. Deng, N. N., Yelleswarapu, M. & Huck, W. T. Monodisperse uni- and multicompartment liposomes. *J. Am. Chem. Soc.* **138**, 7584–7591 (2016).
24. Braha, O. et al. Designed protein pores as components for biosensors. *Chem. Biol.* **4**, 497–505 (1997).
25. Russo, M. J., Bayley, H. & Toner, M. Reversible permeabilization of plasma membranes with an engineered switchable pore. *Nat. Biotechnol.* **15**, 278–282 (1997).
26. Shimizu, Y., Kanamori, T. & Ueda, T. Protein synthesis by pure translation systems. *Methods* **36**, 299–304 (2005).
27. Maloy, S. R., Stewart, V. J. & Taylor, R. K. *Genetic Analysis of Pathogenic Bacteria: A Laboratory Manual*. (Cold Spring Harbor Laboratory Press, 1996).
28. Juers, D. H., Matthews, B. W. & Huber, R. E. *LacZ* β-galactosidase: structure and function of an enzyme of historical and molecular biological importance. *Protein Sci.* **21**, 1792–1807 (2012).
29. Huttunen, K. M., Raunio, H. & Rautio, J. Prodrugs—from serendipity to rational design. *Pharmacol. Rev.* **63**, 750–771 (2011).
30. Elani, Y., Gee, A., Law, R. V. & Ces, O. Engineering multi-compartment vesicle networks. *Chem. Sci.* **4**, 3332–3338 (2013).
31. Elani, Y., Law, R. V. & Ces, O. Protein synthesis in artificial cells: using compartmentalisation for spatial organisation in vesicle bioreactors. *Phys. Chem. Chem. Phys.* **17**, 15534–15537 (2015).
32. Baxani, D. K. et al. Bilayer networks within a hydrogel shell: a robust chassis for artificial cells and a platform for membrane studies. *Angew. Chem. Int. Ed. Engl.* **55**, 14240–14245 (2016).
33. Bubeck, P., Winkler, M. & Bautsch, W. Rapid cloning by homologous recombination in vivo. *Nucleic Acids Res.* **21**, 3601–3602 (1993).

Acknowledgements

This work was supported by a European Research Council Advanced Grant. M.J.B. was funded by Merton College, Oxford, and a Royal Society University Research Fellowship. I.C. was funded by the University of Oxford EPSRC & BBSRC Centre for Doctoral Training in Synthetic Biology [Grant EP/L016494/1], a Clarendon Fund Scholarship and an Oxford-Broomhead Graduate Scholarship.

Author contributions

M.J.B. and H.B. conceived the experiments. M.J.B. and I.C. performed the experiments. All authors wrote the paper.

Competing interests

The authors declare no competing interests.

Additional information

Supplementary information is available for this paper at https://doi.org/10.1038/s42004-019-0244-y.

Correspondence and requests for materials should be addressed to M.J.B.

Reprints and permission information is available at http://www.nature.com/reprints

Publisher's note Springer Nature remains neutral with regard to jurisdictional claims in published maps and institutional affiliations.